CHEMISTRY
A EUROPEAN JOURNAL

DOI: 10.1002/chem.200700428

Dispersion Interactions Govern the Strong Thermal Stability of a Protein

Jiří Vondrášek,*[a] Tomáš Kubař,[a] Francis E. Jenney, Jr.,[b] Michael W. W. Adams,[b] Milan Kožíšek,[c] Jiří Černý,[a] Vladimír Sklenář,[d] and Pavel Hobza*[a]

Abstract: Rubredoxin from the hyperthermophile *Pyrococcus furiosus* (Pf Rd) is an extremely thermostable protein, which makes it an attractive subject of protein folding and stability studies. A fundamental question arises as to what the reason for such extreme stability is and how it can be elucidated from a complex set of interatomic interactions. We addressed this issue first theoretically through a computational analysis of the hydrophobic core of the protein and its mutants, including the interactions taking place inside the core. Here we show that a single mutation of one of phenylalanine's residues inside the protein's hydrophobic core results in a dramatic decrease in its thermal stability. The calculated unfolding Gibbs energy as well as the stabilization energy differences between a few core residues follows the same trend as the melting temperature of protein variants determined experimentally by microcalorimetry measurements. NMR spectroscopy experiments have shown that the only part of the protein affected by mutation is the reasonably rearranged hydrophobic core. It is hence concluded that stabilization energies, which are dominated by London dispersion, represent the main source of stability of this protein.

Keywords: ab initio calculations · hydrophobic core · hydrophobic effect · molecular modeling · NMR spectroscopy

Introduction

Despite research efforts over many years, it is not yet clear how the fundamental mechanisms involved in protein folding act in concert to allow spontaneous folding (in the absence of chaperones) into a stable, three-dimensional structure.[1,2] A particularly efficient way to examine this problem is to analyze proteins from hyperthermophilic organisms, the optimal growth temperatures of which are near and even above 100 °C.[3] Remarkably, proteins from organisms growing in this extreme environment are very homologous to their mesophilic counterparts, and the basis of their hyperthermostability is the sum of numerous small changes rather than any one particular mechanism.[4,5] Perhaps the best studied hyperthermophilic protein is rubredoxin (Rd) from the archaeon *Pyrococcus furiosus* (Pf).[6] Rd is a 53-residue redox-active protein which contains a single Fe atom coordinated by four cysteinyl sulphur residues and is believed to be involved in electron transfer to proteins involved in the detoxification of reactive oxygen species.[7] It is currently the most thermostable protein described, with a predicted melting temperature approaching 200 °C.[8] Although it is not amenable to completely reversible unfolding studies (mainly due to the Fe cofactor), it has been extensively utilized as a model for understanding protein stability, often relative to its counterpart Rd from the mesophile *Clostridium pasteurianum*.[9] A number of hypotheses have been invoked to explain the thermostability of Rd, and data demonstrating several contributions to stability are available, including electrostatic interactions in the β-sheet structure and N terminus,[10] hydrogen bonds,[11] the FeS_4 metal

[a] Dr. J. Vondrášek, Dr. T. Kubař, Dr. J. Černý, Prof. P. Hobza
Institute of Organic Chemistry and Biochemistry
Czech Academy of Sciences and Center for Biomolecules and Complex Molecular Systems, Flemingovo nám. 2
Praha 6 (Czech Republic)
Fax: (+42) 022-041-0320
E-mail: jiri.vondrasek@uochb.cas.cz
pavel.hobza@uochb.cas.cz

[b] Dr. F. E. Jenney, Jr., Prof. M. W. W. Adams
Department of Biochemistry and Molecular Biology
University of Georgia, Athens, GA 30602 (USA)

[c] M. Kožíšek
Department of Biochemistry and Centre for New Antivirals and Antineoplastics
Institute of Organic Chemistry and Biochemistry
Czech Academy of Sciences, Flemingovo nám. 2
Praha 6 (Czech Republic)

[d] Prof. V. Sklenář
Department of Chemistry and National Centre for Biomolecular Research, Masaryk University
Kotlářská 2, Brno (Czech Republic)

Supporting information for this article is available on the WWW under http://www.chemeurj.org/ or from the author.

centre,[12] and packing in the hydrophobic core.[13,14] Some hypotheses have not been substantiated, such as the conformational rigidity of hyperthermophilic versus mesophilic proteins[15] and the difference in temperature dependence of the protein flexibility.[16] In an apo-Rd, lacking the metal cofactor, hydrogen bonds appear to be the major contributor to folding, rather than the hydrophobic core.[17]

All rubredoxins are structurally similar to each other with a tetrahedral array of four cysteine sulphur atoms ligating a single iron atom. They typically consist of 52–54 amino acid residues folded into a short three-stranded antiparallel β-sheet and a number of loops. According to SCOP classification, rubredoxin belongs to a class of small proteins with rubredoxin-like fold and superfamily (see reference [18]).

Stabilization of a protein takes place after a process of arrangement, during which the 3D structure is formed.[2] The ultimate form of a protein molecule and its folding mechanism are two closely related, but not identical, issues. The behavior of mutant variants of the same protein can illuminate the effect on the overall stability, as well as the dynamics of protein folding.[16,19] Such results make it possible to construct a logical framework connecting protein stability and folding. The packing of hydrophobic residues in the core of globular proteins has long been considered a key element in folding and stabilization,[20,21] although there is evidence that this is not the major difference between thermostable proteins and their mesophilic homologues.[22] Rd is a small globular protein containing a distinct hydrophobic core, which may constitute the crucial stabilization element of the structure. The residues forming the core are hydrophobic and tightly packed. Their internal stabilization calculated by using accurate ab initio quantum-chemical methods is strong.[23] The large stabilization energy found inside the core, which originates in the London dispersion energy, led us to speculate about the role of energy (enthalpy) in stabilization and folding. A straightforward extension of this speculation is that the stability (or in this case thermostability) of a protein is directly related to the arrangement of amino acids inside the core and its compactness. This is consistent with several other proposals that it is the internal packing, rather than a hydrophobic effect, that stabilizes the core[24] and may be a key element of thermostability.[21] Any mutation decreasing core stability (in terms of its formation Gibbs energy, or the interaction energy/enthalpy between core components) should be demonstrated by a decrease in thermostability represented by the amount of Gibbs energy necessary for protein denaturation.[25,26] The Gibbs energy of denaturation for various Rd mutants can be dealt with both experimentally and computationally. The latter approach provides deeper insight into the enthalpy–entropy relationships inside the protein and its core. As a benefit, we obtain detailed information about the most structure-stabilizing elements and their role in the energy balance of various Pf Rd mutants. The aim of this study is to elucidate the extreme thermostability of the wild-type (WT) Pf Rd by comparing it to less stable mutants.

Results and Discussion

Interaction energy matrix: We utilized the concept of the "interaction-energy matrix" in order to evaluate an energetic contribution of the hydrophobic core and its most important residues. First, we selected a set of all uncharged amino acids in the WT protein (34 residues) and evaluated the interaction energy between the side chains for each pair formed. In fact, there is one charged residue in Rubredoxin—the Lys 45. Its amine group is not buried and is oriented towards solvent by the charged head. The long aliphatic side chain is nevertheless involved in contact with Phe 48 which also contributes to the overall stability. The reason we did not take the Lys into account is a result of the fact that usually charged amino acids do not occupy the interior of a protein or at least not by their charged terminus and that the hydrophobic core of the studied proteins always contain these amino acids in a similar orientation. The interaction energy matrix was constructed based on pair interaction-energy values between all residues within the set. The values were then summed for each row of the matrix to yield the interaction energy of a single amino acid with the others in the set. The resulting list contained three groups of residues (cf. Figure 1a): 1) Twenty-two had a small total stabilization energy (less than 25 kJ mol^{-1}; shown in red); these were eliminated from further consideration. The limit of 25 kJ mol^{-1} was selected as the strength of an average hydrogen bond, for example, residues which meet the criterion should also possess at least one strong hydrogen bond or more interactions of comparable strength. 2) Four cysteinyl residues forming the FeS_4 centre (shown in yellow); their total interaction energy comes from their mutual interaction rather than from the interactions inside a hydrophobic core, and this was the reason that these were discarded as well. 3) The eight remaining residues subsequently underwent another round of the matrix-generating procedure.

We took water dimmer as a standard of the hydrogen bond strength. The most accurate interaction energy obtained theoretically was determined to be about $\approx$20 kJ mol^{-1}. According to our criteria, this value for purpose of our study was raised to 25 kJ mol^{-1}, which is approximately 5 kcal mol^{-1}. These values are for gas-phase calculations.

Finally, the interaction energy was summed in every row of the final matrix and the amino acids were classified according to this sum. Y10 and I23 exhibited total stabilization energies smaller than 25 kJ mol^{-1} and were thus removed. As a result, we identified the "minimal" hydrophobic core of this protein formed by the following amino acids: W3, Y12, F29, L32, W36 and F48 (see the Supporting Information). The key question to address is how the mutation of these key core residues affects the protein's stability. In our case, we explored the separate mutations of two phenylalanines, F29 and F48.

NMR spectroscopic analysis of Pf Rd mutants: The changes in the three-dimensional structure of three proteins, each

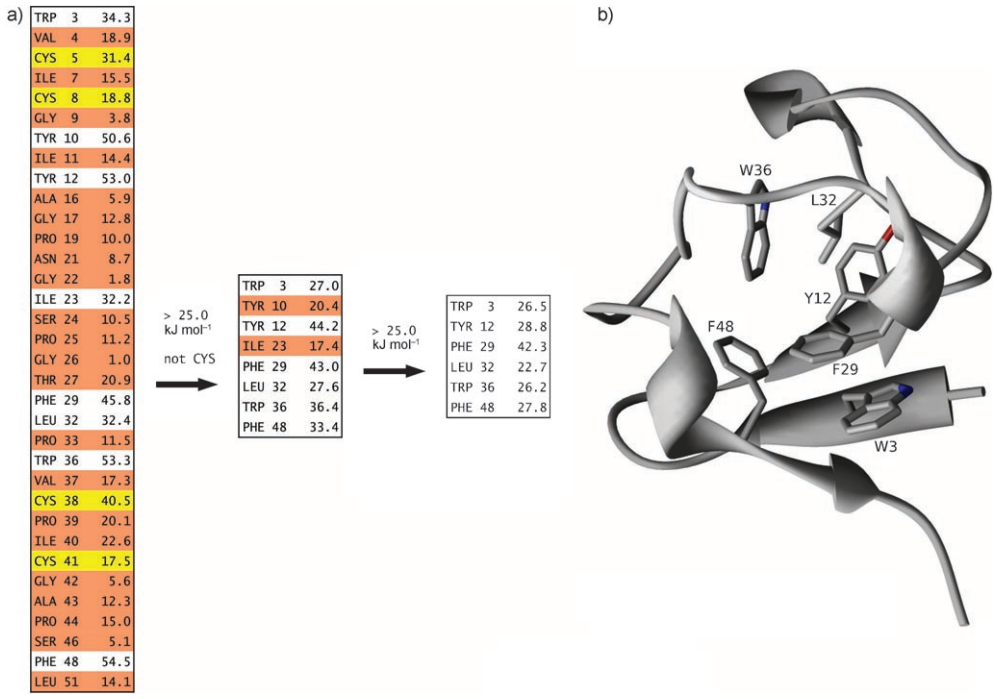

Figure 1. The location of the hydrophobic core (a, left) by the interaction energy matrix procedure and its position in the protein molecule (b, right).

with a single mutation within the minimal hydrophobic core, F29G, F48G and F48A, were examined by ^{1}H and ^{13}C NMR spectroscopy. The presence of high-spin Fe^{3+} ($I=5/2$) in the oxidized Rd protein led to a significant line broadening due to Fermi-contact interactions, making NMR spectroscopic resonances of the nuclei within a distance of approximately 11 Å from the Fe atom invisible. As reported previously for Rd from *C. pasteurianum*,[27] which in its sequence differs only slightly from Pf Rd and shares the same structural topology, the methyl signals of L32 reflect the connection of the loop region to the hydrophobic core. The close proximity of the L33 methyl groups to the aromatic system of W37 (at a distance of ≈3.8 Å) leads to significant shielding of their proton NMR signals. The HD1 protons at a distance of 11.3 Å from a Fe^{3+} atom are more broadened when compared to HD2 at 13.4 Å. The chemical shift values for WT, F29G, F48G and F48A = $\delta = -1.736$, -1.261, -1.464 and -1.260 ppm indicate that the position of L331 with respect to W37 varies only slightly upon mutation. The ^{13}C chemical shifts are found in the range typical for L-methyl group resonances ($\delta = 21.8$–23.3 ppm). HD2 protons provide much sharper signals at $\delta = -0.302$, -0.664, 0.053 and 0.304 ppm for WT, F29G, F48G and F48 A, respectively. Smaller shielding reflects their positions on top of the indole ring as compared to HD1 protons, which are located closer to the benzene ring of W33. Similar values, namely $\delta = -1.76$ and -0.22 ppm for HD1 and HD2, and $\delta = 22.51$ and 21.88 ppm for CD1 and CD2, were reported for the reduced Zn^{2+} form of rubredoxin from *Pyrococcs furiosis*.[9]

The rearrangement of aromatic residues outside the 11 Å distance from Fe^{3+} was monitored by the $^{1}H/^{13}C$ correlation spectra. Closer inspection of the 3D structure shows F29 on the edge of NMR visibility in the presence of the ferric iron atom, with the HE/CE signals broadened beyond the detection limits by Fermi interactions. However, the HD/CD resonance is clearly seen both in WT and F48 A proteins at $\delta =$ 5.55–5.60/130.7 ppm. The HD proton chemical shift reflects the shielding effect of W3, which is less than 4 Å distant. This indicates that structural arrangements in WT and F48 A are very similar. In the F48G mutant, the signal of F29 is not visible. This can be rationalized by the structural modification resulting from the F48G mutation, in which F29 is shifted closer to the Fe^{3+} binding site (and therefore broadened beyond detection by the Fermi interaction with Fe^{3+}), suggesting a contraction of the core. The structural rearrangements of the F48G mutant are corroborated by the NMR spectroscopic signals of W3. The signature resonance of CZ2 at $\delta = 114.4$ ppm and of other aromatic carbons at $\delta = 121$–126.5 ppm disappear completely upon F48G mutation, indicating that in addition to F29, also W3 moves closer to the hydrophobic core, closer to Fe^{3+}. In F48A and F29G mutants, the W3 carbon resonances change very little (by less than $\delta = 1.0$ ppm). The only other aromatic residue visible in the NMR spectra, Y12, is detected by a similar broadening of HE and HD proton resonances in WT and all the mutants. Negligible differences in the resonance line width of the relatively broad HD signal, which is closer to Fe^{3+} than HE (11.5 Å versus 12.7 Å), indicate that the position of Y12 within the structure remains unchanged. The above-described NMR results, therefore, suggest that compactness of the hydrophobic core is maximized as a result of the mutations. However, the overall fold of all mutants is largely unaffected and remains the same for WT and the F29G, F48G and F48A mutants.

Effect of mutations on melting temperatures: Thermal unfolding of WT and the F29I, F29G, F48A and F48G mutants of Pf Rd was measured with a VP-DSC calorimeter. Figure 2a presents the calorimetric thermograms showing the excess heat capacity as a function of temperature. All mutant Rds, except for F48A, showed only a change in heat capacity (similar to the report of Bonomi et al.[13]). The transition temperatures were 55.5 (F29I), 47.5 (F29G), 63 (F48 A) and 62.5 °C (F48G). In stark contrast, WT exhibited a denaturation profile extending beyond 100 C. The effects of the single amino acid mutations on the conformational stability of the protein are, therefore, considerable and WT is dramatically more stable than any of the mutants. The F29G mutant has the lowest transition temperature or, in other words, the largest decrease in stability. The effect was smaller in the F29I protein, and the smallest, yet still very significant, decrease of transition temperature was exhibited by changing F48 either to alanine or glycine.

Gibbs free energy of folding from simulation: The change of melting temperature in the mutant relative to the WT is obviously related to a change in protein stability, and this phenomenon can be quantified by the change in unfolding Gibbs energy. Because of the small difference in the 3D structure of the Rd mutants indicated by the NMR spectra, we can approach the unfolding Gibbs energy computationally with the molecular dynamics–thermodynamic integration technique (MD-TI). We calculated the change of unfolding Gibbs energy upon the mutation of WT by using the force field of Cornell et al.[28] As shown in Table 1, the largest decrease of unfolding Gibbs energy ($\Delta\Delta G$) is found for F29G, followed by F29I; both F48A and F48G possess considerably smaller $\Delta\Delta G$ values of -15 to -20 kJ mol^{-1}. The $\Delta\Delta G$ values reflect the decrease of melting temperature accompanying the mutation of Rd (cf. Table 1 and Figure 2b). This indicates that changes in the core correlates with the decrease of thermal stability for the studied Pf Rd mutants.

Table 1. The measured and calculated characteristics of Pf Rd and the mutants (sorted by decreasing thermal stability).

Protein	T_m [°C][a]*	$\Delta\Delta G$ [kJ mol^{-1}][b]	$\Delta\Delta E^{stab}$ [kJ mol^{-1}][c]	$\Delta\Delta E^{disp}$ [kJ mol^{-1}][d]	$-T\Delta\Delta S$ [kJ mol^{-1}][e]
WT	>100	0	0	0	0
F48A	63.0	-15.3 ± 4.4	-11.1	-25.5	-19.2
F48G	62.5	-18.6 ± 5.3	-13.4	-27.6	-27.8
F29I	55.5	-32.4 ± 6.0	-11.9	-27.2	-30.9
F29G	47.5	-41.4 ± 4.6	-41.2	-74.3	-31.9

[a] Melting temperature; * = determined experimentally. [b] Difference of Gibbs energy of unfolding with respect to WT by means of the MD-TI method. [c] Difference of total stabilization energy in the hydrophobic core with respect to WT evaluated by the DFT-D method. [d] The dispersion-energy component of $\Delta\Delta E^{stab}$ corresponding to the empirical part of DFT-D. [e] Difference of entropy of unfolding with respect to WT by means of normal-mode analysis.

Enthalpy and entropy contributions to folding: We have previously demonstrated the importance of stabilization energy within the Rd hydrophobic core.[23] A natural extension of this idea is to ask whether the (weaker) thermal stability of various mutants corresponds to the (decreased) stabilization energy within the hydrophobic core. We evaluated the interaction energy inside the core containing six amino acid residues by using the "interaction-energy matrix" method for the WT and all the corresponding mutants; for these calculations, we applied the density-functional theory approach augmented by the empirical correction term accounting for dispersion energy. This technique, which covers the London dispersion energy correctly, yields an accurate stabilization energy that is in good agreement with that predicted by most accurate quantum-chemical methods[29] (for details, see the section on interaction energy calculations and the model of amino acid side chains in materials and methods). Furthermore, the portion of stabilization energy which may be attributed to dispersion interactions can be estimated. Table 1 shows the relative stabilization energy of the core for the mutant proteins with respect to WT as well as the dispersion-energy component thereof. The studied mutations decrease the stabilization energy by 11 to 41 kJ mol^{-1}, which agrees well with the drop of melting temperature (cf. Table 1 and Figure 2b). This indicates that the attractive side-chain interactions play a crucial role in the stability of the protein. Table 1 also presents the change of the dispersion contribution to stabilization energy (column 4), and we can see that this quantity decreases even more markedly upon mutation. Therefore, we can conclude that the stabilization energy originates from the London dispersion interaction.

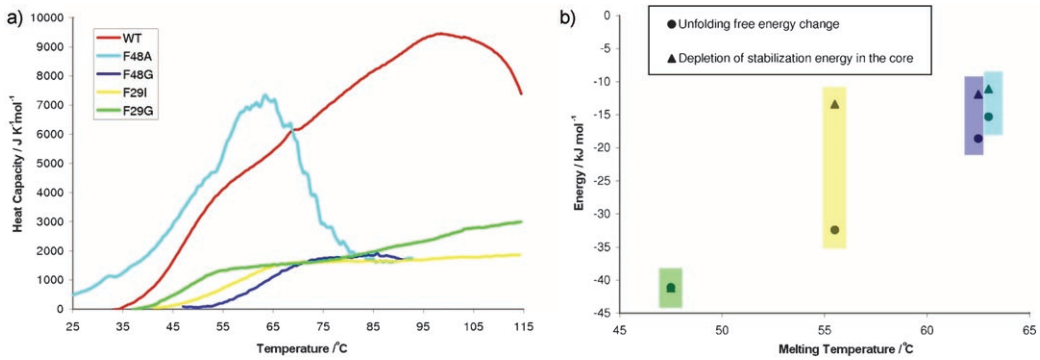

Figure 2. The thermal denaturation of Pf Rd and its mutants (a) and the calculated thermodynamic parameters (b).

To consider all the contributions of the Gibbs energy of denaturation, the entropic part must be taken into account. The normal-mode analysis (with the force field by Cornell et al.[28]) was performed for WT as well as for all the mutants to estimate the vibrational entropy. The results are presented in Table 1 in terms of the unfolding entropy change with respect to WT. It is clear that the unfolding entropy change is another unfavorable contribution by the mutation. The calculated entropy changes suggest an increase of hydrophobic core stiffness upon mutation. This is in concord with the NMR spectroscopy results and indicates a rearrangement of the core in order to maintain the compactness. It is proposed that the hydrophobic core of WT Rd is balanced to exhibit both maximum stabilization energy and maximum conformational freedom. Upon mutation, the core tends to minimize the depletion of stabilization energy by the structural reorganization of some residues and becomes stiffer. Consequently, a part of the conformational freedom (and thus entropy) is lost. This is reflected by a positive $-T\Delta\Delta S$ with respect to WT.

Discussion

The hydrophobic core and its unique spatial arrangement is the part of Rd that contributes notably to its unusual thermal stability. This fact is supported by the experimental as well as theoretical results. The relative unfolding Gibbs energy values obtained by the MD method agree with the course of thermal denaturation of the mutant proteins with respect to the WT version. Moreover, we are able to trace the overall stability reflected in the relative stabilization energy of the core, which also agrees with the melting temperature of the studied proteins. This results from the weakening of the interactions between the amino acid side chains composing the hydrophobic core in the mutants relative to WT. Normal mode analysis provides an insight into the thermodynamics of the protein and shows that the entropy of the protein is reduced upon mutation inside the core as a consequence of the core rearrangement, and this is another destabilizing factor. The major structural differences between the WT Rd and its mutants is localized in the core through particular side-chain interactions. The overall structure of the molecule is retained, corroborated by the NMR spectroscopic data. We conclude that the high stability content of Pf Rd results substantially from the highly favorable interaction of amino acid side chains inside the hydrophobic core of the protein, which originates in its entirety in the London dispersion interactions.

We can speculate that the loss of favorable interactions caused by a mutation inside the core is partially compensated by a spatial rearrangement of the core, and this occurs at the cost of configurational entropy. Supported by the NMR spectroscopic experiment and the results of calculations, we assumed that structure and stability can be a reflection of the energy content. This concept can have an impact on various protein-related issues including stability and dynamics. We believe that this is a serious physically relevant step to the resolution of the protein-folding problem as well as prediction of proteins tertiary structure.

Experimental Section

Protein purification and differential scanning calorimetry: Site-directed mutagenesis of the Pf Rd gene was performed by using the QuikChange kit (Stratagene, La Jolla, CA). The recombinant forms of Rd mutant proteins were expressed and the proteins purified as previously described.[6] Thermal denaturation experiments were performed on a high precision VP-DSC differential scanning calorimeter (MicroCal, USA). The protein solutions after purification were dialyzed against 50 mM Tris-HCl, pH 7.4 and diluted with the same buffer to concentrations of between 0.4 and 0.45 mM (2.3 and 2.6 mg mL^{-1}). Protein concentration was determined by the HPLC total amino acid analysis. The protein samples and reference solution (buffer) were degassed and carefully loaded into the cells to avoid bubble formation. These samples were heated to 115 °C at a scan rate of 60 °C per hour. The observed denaturation profiles, excess heat capacity versus temperature, were superimposed after baseline correction by using Origin 5.0 software (Microcal).

NMR spectroscopy: The NMR spectra were measured on a 600 MHz NMR spectrometer Bruker Avance equipped with the triple-resonance 5 mm TCI HCN cryoprobe. 0.4 mM samples of WT, F29G, F48G and F48 A mutants were dissolved in a phosphate buffer (pH 7.4) with 90 % H_2O and 10 % D_2O. ^{1}H NMR 1D spectra were obtained with water presaturation under standard acquisition conditions. 2D ^{1}H-^{13}C HSQC experiments were acquired at 303 K with 96 scans per FID, 2560 and 380 complex points in ^{1}H and ^{13}C dimensions, relaxation delay 1.2 s when using a spectral width of $\delta = 16$ (^{1}H) and 80 ppm (^{13}C NMR spectra). The aliphatic and aromatic parts were acquired independently with the ^{13}C carrier frequency set to $\delta = 40$ and 120 ppm, respectively. The assignment of the NMR signals was based on the ^{1}H and ^{13}C data reported for the Zn^{2+} form of the wild-type Rd[9] and on a comparison with the 3D structure of oxidized Fe^{3+} Pf Rd obtained by X-ray crystallography[30] (PDB ID 1CAA).

Gibbs energy calculations: The folding Gibbs energy difference between various mutants of Pf Rd was determined by means of molecular dynamics–thermodynamic integration (MD-TI) calculations. A direct calculation of the folding Gibbs energy of protein (processes F1 and F2 in Scheme 1) is quite difficult, introducing large uncertainty. On the other hand, the calculation of the Gibbs energy difference for the "alchemical" change of one amino acid side chain into another (processes M1 and M2 in Scheme 1) is both easier and accurate enough provided there is little difference between the two structures. As Gibbs energy is a state function, the following equation holds:

$$\Delta\Delta G = \Delta G(\mathrm{F2}) - \Delta G(\mathrm{F1}) = \Delta G(\mathrm{M2}) - \Delta G(\mathrm{M1})$$

We performed the MD-TI calculations for the "alchemical" change of amino acid side chain twice: first in the folded protein and then in the free amino acid dissolved in water to approximate the mutation in denaturated protein. Subsequently, the folding Gibbs energy difference was obtained as the difference of the two ΔG values calculated.

We used the GROMACS 3.1.4 molecular simulation package[31,32] with the Cornell et al. force field,[28] which describes both intra- and intermolecular interactions inside biological systems with relevant accuracy. To control both equilibration and uncertainty, the reverse cumulative aver-

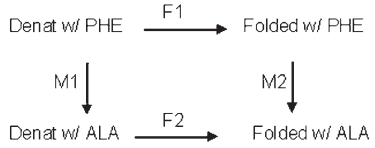

Scheme 1. The thermodynamic cycle.

aging (RCA) procedure[33] was adopted and implemented in GROMACS (for computational details, cf. for example, our recent article in reference [34]).

To avoid unstable simulations and incorrect free-energy accumulation arising from singularities in the van der Waals and Coulomb potential energy terms, soft-core potential energy scaling[35] was used systematically.

The simulations were divided into so-called windows with fixed values of the coupling parameter *l*. By using RCA, the data-collection stage commenced when the system was equilibrated at an 85% confidence level and was terminated when the uncertainty of the free-energy derivative dropped below 6 kJ mol^{-1}.

Interaction-energy calculations and the model of amino acid side chains: Our goal was to quantify the protein stabilization that stems from the favorable interactions of the amino acid side chains. Therefore, only those side chains starting with the C_α atom were considered in the calculations of interaction energy. For example, the amino acids alanine and phenylalanine are represented by ethane and ethylbenzene, respectively.

The interaction (stabilization) energy of an amino acid pair was calculated as the difference of the energy of the pair and the sum of the energy of both amino acids forming the pair. The energy of the pair and that of its components were obtained by using two approaches: 1) In the process of core localization it was the molecular-mechanics force field of Cornell et al.,[28] while (2) to receive more accurate values of interaction energy, the density-functional theory approach augmented with the empirical correction term accounting for dispersion energy[29] was employed. The latter methodology is based on a DFT calculation with the TPSS density functional and the TZVP basis set. The method yields accurate interaction energies for the various molecular clusters, which are well comparable with highly correlated CCSD(T) calculations performed at the complete basis set limit. Moreover, the method exhibits negligible values of the basis-set-superposition error.

The geometry of the protein molecule was taken from the protein databank (PDB ID 1BRF) for the wild-type Rd and from the MD-TI simulations in the case of all the mutants. The structures were energy-minimized twice: in the aqueous environment and, subsequently, in vacuo. These minimizations were performed by using the force field by Cornell et al.[28]

Normal-mode analysis: Vibrational (normal-mode) analysis was used to estimate the change of entropy and zero-point vibrational energy (ZPVE) accompanying the folding of a protein. The Hessian matrix in mass-weighted coordinates and its eigenvalues were calculated for the energy-minimized structure of every protein molecule in vacuo. These calculations were performed with the Cornell et al. force field[28] by using the Gromacs 3.2 package. The vibrational partition function was then calculated and used to estimate the vibrational entropy and ZPVE. We assumed the change of entropy of translation and rotation in the course of protein folding to differ negligibly for all the variants of Rd and thus we did not evaluate it. The same calculations were performed for a set of isolated amino acids (F, I, A and G) to estimate the difference of entropy of the unfolded protein.

Acknowledgements

This work was supported by grants from the Czech Science Foundation (grants nos. 203/06/1727 and 203/05/H001), the Grant Agency of the Academy of Sciences of the Czech Republic (grant no. A400550510), the Ministry of Education, Youth and Sports of the Czech Republic (grant nos. LC512, MSM0021622413 and 1M0508) and by a grant from the National Institutes of Health (no. GM 60239).

[1] S. Ventura, L. Serrano, *Proteins Struct. Funct. Bioinf.* **2004**, *56*, 1–10.
[2] M. Levitt, M. Gerstein, E. Huang, S. Subbiah, J. Tsai, *Annu. Rev. Biochem.* **1997**, *66*, 549–579.
[3] R. Huber, H. Huber, K. O. Stetter, *FEMS Microbiol. Rev.* **2000**, *24*, 615–623.
[4] A. Szilagyi, P. Zavodszky, *Structure* **2000**, *8*, 493–504.
[5] I. N. Berezovsky, E. I. Shakhnovich, *Proc. Natl. Acad. Sci. USA* **2005**, *102*, 12742–12747.
[6] F. E. Jenney Jr. , M. W. Adams, *Methods Enzymol.* **2001**, *334*, 45–55.
[7] A. M. Grunden, F. E. Jenney Jr. , K. Ma, M. Ji, M. V. Weinberg, M. W. Adams, *Appl. Environ. Microbiol.* **2005**, *71*, 1522–1530.
[8] D. M. LeMaster, J. Tang, D. I. Paredes, G. Hernandez, *Biophys. Chem.* **2005**, *116*, 57–65.
[9] C. M. Bougault, M. K. Eidsness, J. H. Prestegard, *Biochemistry* **2003**, *42*, 4357–4372.
[10] S. Kumar, R. Nussinov, *Chembiochem* **2004**, *5*, 280–290.
[11] K. Kurihara, I. Tanaka, T. Chatake, M. W. Adams, F. E. Jenney Jr., N. Moiseeva, R. Bau, N. Niimura, *Proc. Natl. Acad. Sci. USA* **2004**, *101*, 11215–11220.
[12] F. Bonomi, M. K. Eidsness, S. Iametti, D. M. Kurtz Jr. , S. Mazzini, A. Morleo, *J. Biol. Inorg. Chem.* **2004**, *9*, 297–306.
[13] F. Bonomi, D. Fessas, S. Iametti, D. M. Kurtz Jr. , S. Mazzini, *Protein Sci.* **2000**, *9*, 2413–2426.
[14] B. Anil, S. Sato, J. H. Cho, D. P. Raleigh, *J. Mol. Biol.* **2005**, *354*, 693–705.
[15] A. Grottesi, M. A. Ceruso, A. Colosimo, A. Di Nola, *Proteins Struct. Funct. Gen.* **2002**, *46*, 287–294.
[16] D. M. LeMaster, J. Tang, D. I. Paredes, G. Hernandez, *Proteins Struct. Funct. Bioinf.* **2005**, *61*, 608–616.
[17] E. R. Zartler, F. E. Jenney Jr. , M. Terrell, M. K. Eidsness, M. W. Adams, J. H. Prestegard, *Biochemistry* **2001**, *40*, 7279–7290.
[18] http://scop.mrc-lmb.cam.ac.uk/scop/.
[19] C. G. Benitez-Cardoza, K. Stott, M. Hirshberg, H. M. Went, D. N. Woolfson, S. E. Jackson, *Biochemistry* **2004**, *43*, 5195–5203.
[20] G. A. Lazar, T. M. Handel, *Curr. Opin. Chem. Biol.* **1998**, *2*, 675–679.
[21] S. P. Pack, Y. J. Yoo, *Int. J. Biol. Macromol.* **2005**, *35*, 169–174.
[22] A. Karshikoff, R. Ladenstein, *Protein Eng.* **1998**, *11*, 867–872.
[23] J. Vondrasek, L. Bendova, V. Klusak, P. Hobza, *J. Am. Chem. Soc.* **2005**, *127*, 2615–2619.
[24] J. Chen, W. E. Stites, *Biochemistry* **2001**, *40*, 15280–15289.
[25] M. Vlassi, G. Cesareni, M. Kokkinidis, *J. Mol. Biol.* **1999**, *285*, 817–827.
[26] G. S. Ratnaparkhi, R. Varadarajan, *Biochemistry* **2000**, *39*, 12365–12374.
[27] F. Bonomi, A. E. Burden, M. K. Eidsness, D. Fessas, S. Iametti, D. M. Kurtz Jr. , S. Mazzini, R. A. Scott, Q. Zeng, *J. Biol. Inorg. Chem.* **2002**, *7*, 427–436.
[28] W. D. Cornell, P. Cieplak, C. I. Bayly, I. R. Gould, K. M. Merz, D. M. Ferguson, D. C. Spellmeyer, T. Fox, J. W. Caldwell, P. A. Kollman, *J. Am. Chem. Soc.* **1995**, *117*, 5179–5197.
[29] P. Jurecka, J. Cerny, P. Hobza, R. S. Salahub, *J. Comput. Chem.* **2007**, *28*, 555–569.
[30] M. W. Day, B. T. Hsu, L. Joshuator, J. B. Park, Z. H. Zhou, M. W. W. Adams, D. C. Rees, *Protein Sci.* **1992**, *1*, 1494–1507.
[31] D. van der Spoel, E. Lindahl, B. Hess, G. Groenhof, A. E. Mark, H. J. Berendsen, *J. Comput. Chem.* **2005**, *26*, 1701–1718.
[32] E. Lindahl, B. Hess, D. van der Spoel, *J. Mol. Model.* **2001**, *7*, 306–317.
[33] W. Yang, R. Bitetti-Putzer, M. Karplus, *J. Chem. Phys.* **2004**, *120*, 2618–2628.
[34] T. Kubar, M. Hanus, F. Ryjácek, P. Hobza, *Chem. Eur. J.* **2006**, *12*, 280–290.
[35] J. Ruiz-Sanz, V. V. Filimonov, E. Christodoulou, C. E. Vorgias, P. L. Mateo, *Eur. J. Biochem.* **2004**, *271*, 1497–1507.

Received: March 19, 2007
Revised: July 13, 2007
Published online: August 15, 2007

